

## LETTER TO THE EDITOR

## Dynamical stabilization of classical multi-electron targets against autoionization

Tihamér Geyer<sup>1</sup> and Jan M Rost<sup>2</sup><sup>1</sup> Department of Chemical Physics, Weizmann Institute of Science, Rehovot 76100, Israel<sup>2</sup> Max-Planck-Institute for the Physics of Complex Systems, Nöthnitzer Straße 38, D-01187 Dresden, Germany

Received 22 December 2002

Published 10 February 2003

Online at [stacks.iop.org/JPhysB/36/L107](http://stacks.iop.org/JPhysB/36/L107)**Abstract**

We demonstrate that a recently published quasiclassical Møller type approach (Geyer and Rost 2002 *J. Phys. B: At. Mol. Opt. Phys.* **35** 1479) can be used to overcome the problem of autoionization, which arises in classical trajectory calculations for many-electron targets. In this method, the target is stabilized dynamically by a backward–forward propagation scheme. We illustrate this refocusing and present total cross sections for single and double ionization of helium by electron impact.

Classical trajectory descriptions of atomic collisions and ionization processes have a long history, dating back to the pioneering work of Abrines and Percival [1]. The method has never become a mainstream tool, but has been used over the years for a variety of collision systems. This so-called CTMC (classical trajectory Monte Carlo) method was originally formulated with macroscopic point particles, scaled down to the dimensions of a real hydrogen atom, but it can be derived as a discretized treatment of the system's Liouville equation, too (see, e.g., [2]). In the hydrogen target, for which CTMC was formulated initially, the single electron orbits around the nucleus on a Kepler ellipse. If this concept is extended, the resulting many-electron atom is highly unstable: the electrons exchange energy and finally one of them ends up in a very tightly bound orbit and all the others are kicked out of the atom. This process is called autoionization, as it does not need any external perturbation. Therefore, it is practically impossible to use such a classical many-electron atom as a target in a CTMC calculation—it dissolves on its own before the approaching projectile has any chance to interact with it.

Various attempts have been made to stabilize classical many-electron atoms, so that they could be used in ionization and excitation calculations. These attempts range from neglecting the target electrons' interaction completely in the independent electron model, through highly symmetric initial configurations, which autoionize slightly more slowly [3], up to additional momentum dependent potentials to incorporate the uncertainty relation [4]. These ansätze are then usable in CTMC calculations, but they either describe a modified scattering system or lead to inconsistencies.

Motivated by these and other shortcomings of the standard CTMC method, we recently proposed a quasiclassical description for particle impact ionization, which is derived as an approximation to the quantum mechanical description [5]: the Møller formulation of the quantum scattering operator is translated into the Wigner phase space formalism [6] and finally approximated by setting  $\hbar \rightarrow 0$ . The approximation procedure itself is well established and the resulting method is technically very similar to CTMC, as in both treatments the cross sections are evaluated by propagating classical trajectories. But nevertheless there are two fundamental differences:

- (i) the phase space description of the target's initial state is derived free of ambiguity from the quantum mechanical wavefunction without the need to artificially introduce quantization recipes for many-electron atoms and
- (ii) the Møller form of the scattering operator translates into a classical backward–forward–backward propagation scheme, which stabilizes arbitrary initial distributions.

With this ansatz we could calculate fully differential cross sections for electron impact ionization of hydrogen, which essentially reproduce the experimental results over a wide range of energies and geometries [5]. We will now demonstrate that this approximation can also deal with an autoionizing classical helium target.

As mentioned above our quasiclassical approximation is derived as the  $\hbar = 0$  limit of the Wigner formulation of the quantum scattering operator  $\hat{S}$  in the Møller form (for details, please see [5] and references therein):

$$\hat{S} = \Omega_-^\dagger \Omega_+ \quad \text{with } \Omega_\pm = \lim_{t \rightarrow \mp\infty} U^\dagger(t) U_0(t).$$

The propagators  $U(t) = \exp[-iHt]$  and  $U_0(t)$  finally translate into solving Hamilton's equations of motion for each of the (multi-dimensional) discretization points of the initial distribution

$$\rho(t=0) = \rho^i(x, p) = \mathcal{N} \sum_n w_n \delta(x - x_n) \delta(p - p_n).$$

The weights  $w_n$  are the values of the  $\hbar = 0$  limit of the Wigner transform  $w^i$  of the initial state wavefunction at the discretization point:  $w_n = w^i(x_n, p_n)$ . It can be shown that the Wigner transform is only one special case to select the initial conditions; by modifying the underlying correspondence rule, nearly arbitrary translations between wavefunctions and phase space distributions can be constructed [7, 8]. We will later use this freedom to calculate cross sections with a simpler initial state distribution.

According to the Møller scheme each trajectory is first propagated backward in time under the asymptotic initial Hamiltonian  $H_0^i$ , i.e., with the interaction between target and projectile switched off. If not denoted otherwise, we will in the following use atomic units. Its form is then

$$H_0^i = \frac{p_p^2}{2} + \frac{p_1^2}{2} - \frac{Z}{r_1} + \frac{p_2^2}{2} - \frac{Z}{r_2} + \frac{1}{|r_1 - r_2|}. \quad (1)$$

The subscript  $p$  denotes the projectile, whereas the target electrons are labelled with 1 and 2. The nucleus is set to have an infinite mass.

When projectile and target are separated far enough, denoted symbolically by  $t = -\infty$ , the interaction is switched on and the trajectory evolves forward again under the full Hamiltonian  $H$  through the collision at  $t = 0$  and on, until the fragments are well separated again. Then the fragments are brought back from  $t = \infty$  independently, i.e., with the asymptotic final  $H_0^f$ , to the initial time  $t = 0$ . If the initial state is unstable under the classical propagation, as is the case with a helium target, then it autoionizes already during the first backward propagation.

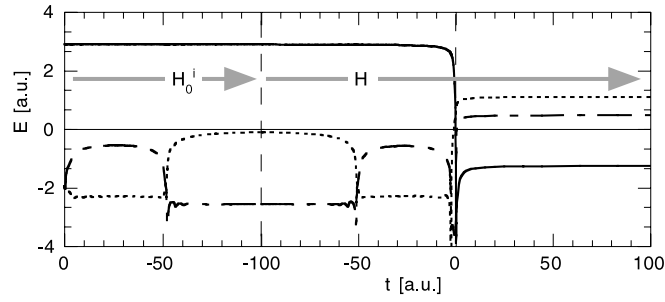


**Figure 1.** One-electron energies of the three electrons in the course of an example trajectory. The two target electrons (broken curves) each start at  $-1.94$  au. The propagation starts backwards with  $H_0^i$  (1) until  $t = -100$  au and is then reversed. The forward propagation is performed with the full Hamiltonian,  $H$ . The energy of the projectile (solid curve) is shifted from  $E_p = 2$  keV to  $IP_1 + IP_2$ . For further explanations please see the text.

When the projectile–target interaction is added at the turning point  $t = -\infty$ , it is negligible first; the forward propagation effectively undoes the autoionization and the projectile encounters the refocused target in nearly its initial state. The autoionization still takes place, but now it is shifted away to  $t < 0$ , where it has no influence on the actual collision dynamics, which takes place around  $t = 0$ . There is consequently no longer any need to neglect some part of the interactions or to introduce additional stabilizing potentials.

In a quantum treatment, the first backward propagation only contributes a phase shift, as the initial state is an eigenstate of  $H_0^i$ . The cross sections remain unchanged if it is neglected. In the classical approximation, though, the target is not stationary during the backward and the forward propagations; but, if both are performed, most of the error due to the approximation cancels, and the target is effectively stationary with respect to the central time,  $t = 0$ : it is this point in time, where the initial conditions are set up, that the collision takes place and where finally the cross sections are extracted.

The stabilizing effect of this Møller type backward–forward–backward scheme is demonstrated in figure 1: there, the one-electron energies  $E_n = \frac{p_n^2}{2} - \frac{2}{r_n}$ ,  $n = p, 1, 2$ , of the projectile (solid curve) and the two target electrons (broken curves) during one trajectory, i.e., the evolution of one single discretization point, are plotted against the propagation time. The interaction energies between the electrons are not included. The propagation starts at  $t = 0$  and first proceeds backwards, here up to  $t = -100$  au, under  $H_0^i$  (1), i.e., with target and projectile independent of each other. Then, the propagation reverses and the full  $H$  is used to propagate back to  $t = 0$  and through the scattering event. The plot ends at ‘ $+\infty$ ’, which is  $t = 100$  au here. In the final backward propagation the electrons are independent of each other, i.e., their energies do not change any more. Hence, we do not show this part of the trajectory in figure 1.

The target electrons were started in a symmetric configuration for the trajectory of figure 1. Within less than one period one of them is kicked into a large orbit, from which it returns after about 50 au and kicks out the other electron. After the propagation is reversed, it is clearly seen that for most of the now-following forward propagation the energies of the target electrons ‘rewind’ the backward propagation, i.e., the broken lines are symmetric with respect to  $t = -100$  au. In other cases (not shown here), one of the electrons is even kicked out of the atom to a positive energy and only comes back due to the reversed propagation. The projectile’s energy of  $E_p = 2$  keV = 73.5 au is shifted in the plot by  $E_p - (IP_1 + IP_2)$ , i.e., the projectile is plotted to start at the negative energy of the target.  $E_p$  is constant during the

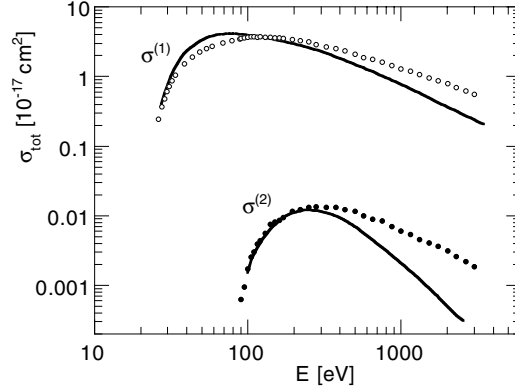


**Figure 2.** Total cross sections  $\sigma^{(1)}$  for single and  $\sigma^{(2)}$  for double ionization: comparison of our results (solid curves) with the experimental data of Shah *et al* [9] (open and filled circles).

backward and most of the forward propagation. It only starts to change shortly before  $t = 0$ , when the interaction with the target electrons increases. Then, the symmetry of the target electron energy trajectories against  $t = -100$  au is broken, and all three electron–electron interactions together determine the dynamics of the actual ionization event. In this plot both electrons are lifted to positive energies, i.e., double ionization occurs.

Another difficulty in the classical description arises from the fact that the final state is normally of well defined energy. Since the Hamiltonian is conservative, only that part of the initial Wigner distribution which lies on this energy shell contributes. Consequently, the quantum distribution character of the initial state is lost. To overcome this problem, we proposed in [5] to evaluate the cross sections in terms of the energy transfer, which, for hydrogen targets, is equivalent to only looking at the projectile’s energy.

With the helium target, a trajectory contributes to double ionization when the projectile’s energy loss  $\Delta E_p$  is bigger than the sum of the ionization potentials  $IP_1$  and  $IP_2$  of the target *and* when both the target electrons have gained at least half of the total binding energy:

$$-\Delta E_p > IP_1 + IP_2 \quad \text{and} \quad \Delta E_1, \Delta E_2 > \frac{IP_1 + IP_2}{2}. \quad (2)$$

A contribution to single ionization is consequently defined by

$$-\Delta E_p > IP_1, \quad \Delta E_1 > \frac{IP_1 + IP_2}{2} \quad \text{and} \quad \Delta E_2 < \frac{IP_1 + IP_2}{2}. \quad (3)$$

Of course, this test has to be performed with the target electrons’ energy transfers  $\Delta E_1$  and  $\Delta E_2$  swapped, too.

To verify the conditions (2) and (3) for double and single ionization, we need the initial and the corresponding final state wavefunctions. The initial state is the same in all cases. We are therefore, as in the experiment, able to extract *all* physically feasible cross sections from the same set of final values of the propagated trajectories.

As a first test of the performance and consistency of our approach with the helium target, we calculated the absolute total cross sections  $\sigma^{(1)}$  for single and  $\sigma^{(2)}$  for double ionization. They are compared to absolute measurements by Shah *et al* [9] in figure 2.

For this first calculation, we have used a simple initial distribution obtained from a product wavefunction for the ground state of the helium target,

$$\psi(r_1, r_2) = \frac{\tilde{Z}^3}{\pi} \exp(-\tilde{Z}r_1) \exp(-\tilde{Z}r_2) \quad (4)$$

with effective nuclear charge  $\tilde{Z} = \frac{27}{16}$  [10]. Each of the single-electron wavefunctions is then translated into a phase space distribution by multiplying its densities in coordinate and momentum space [8]. Both the wavefunction (4) and the resulting phase space distribution have a total energy of  $E = -2.85$  au, slightly less than the experimental value of  $-2.904$  au.

The single-ionization cross section,  $\sigma^{(1)}$ , reproduces the measured data on the level of accuracy that is typical for a single-electron CTMC calculation, see, e.g., [3]: the maximum occurs at a lower energy and is slightly higher than the experiment, while the high energy behaviour follows the classical  $1/E$  decay [11]. The explicit treatment of both target electrons and of all interactions cannot, of course, reintroduce quantum effects like tunnelling. On the other hand, the accessible phase space volume is much bigger than with only one active electron, and one might fear that the dynamics ‘strays away’ from the reaction path of single ionization, completely distorting the cross section—which obviously does not happen. In fact, our result is in good agreement with an nCTMC calculation by Schultz *et al* [3].

The more interesting result is, of course, the double-ionization cross section  $\sigma^{(2)}$ : figure 2 shows the first classical trajectory result ever, in which the dynamics according to the correct full Hamiltonian without any modifications or additions was solved—simultaneously both for  $\sigma^{(1)}$  and  $\sigma^{(2)}$ . The double-ionization cross section has two regions of different correspondence with the experiment: for high energies it decays as  $1/E^2$ , much faster than the experimental data. This suggests that in our calculation in the high energy regime both electrons are ionized independently, each contributing a classical factor of  $1/E$ , and not in a sequential event, which should decay approximately as  $\sigma^{(1)}$  [12]. For impact energies below 250 eV, on the other hand, the experiment is reproduced remarkably well, both in shape and in magnitude. In that region no microscopic quantum mechanical explanation has been proposed yet. It is known, though, that right above the threshold the final state is defined only by the long range and long time dynamics of the outgoing electrons, which can be well described classically [13, 14]. The good agreement between our classical result and the measured data shows that, up to a total energy of about twice the total binding energy of the helium target, the main reaction paths are the classical ones.

In this letter, we have demonstrated for the first time that electron impact ionization of a two-electron atom, i.e., helium, can be calculated within a CTMC framework with the full, unmodified helium Hamiltonian. This has been achieved with a quasiclassical Møller formalism: the propagation scheme refocuses and stabilizes the autoionizing target. The total cross sections, extracted from the energy transfer, compare well with the experiment, to within the limitations of the classical approximation.

The next, more demanding, level of tests will be to compare the differential cross sections to experimental results and finally to understand the dynamics of double ionization in the low energy regime.

This work was funded by the Israel Science Foundation.

## References

- [1] Abrines R and Percival I C 1966 *Proc. Phys. Soc.* **88** 861
- [2] Keller S, Ast H and Dreizler R M 1993 *J. Phys. B: At. Mol. Opt. Phys.* **26** L737
- [3] Schultz D R, Meng L and Olson R E 1992 *J. Phys. B: At. Mol. Opt. Phys.* **25** 4601
- [4] Kirschbaum C L and Wilets L 1980 *Phys. Rev. A* **21** 834
- [5] Geyer T and Rost J M 2002 *J. Phys. B: At. Mol. Opt. Phys.* **35** 1479
- [6] Wigner E 1932 *Phys. Rev.* **40** 749
- [7] Mehta C L 1964 *J. Math. Phys.* **5** 677
- [8] Cohen L 1966 *J. Math. Phys.* **7** 781

- [9] Shah M B, Elliot D S, McCallion P and Gilbody H B 1988 *J. Phys. B: At. Mol. Opt. Phys.* **21** 2751
- [10] Hylleraas E A 1929 *Z. Phys.* **54** 347
- [11] Thomson J J 1912 *Phil. Mag. S. 6* **23** 449
- [12] Rejoub R, Lindsay B G and Stebbings R F 2002 *Phys. Rev. A* **65** 042713
- [13] Wannier G H 1953 *Phys. Rev.* **2** 817
- [14] Rost J M 1994 *Phys. Rev. Lett.* **72** 1998